Magn Reson Mater Phy (2016) 29:843–852
DOI 10.1007/s10334-016-0574-z

RESEARCH ARTICLE

Accelerated visualization of selected intracranial arteries by cycled super-selective arterial spin labeling

Thomas Lindner[1] · **Naomi Larsen**[1] · **Olav Jansen**[1] · **Michael Helle**[2]

Received: 5 March 2016 / Revised: 10 June 2016 / Accepted: 13 June 2016 / Published online: 29 June 2016

Abstract
Objective To accelerate super-selective arterial spin labeling (ASL) angiography by using a single control condition denoted as cycled super-selective arterial spin labeling.
Materials and methods A single non-selective control image is acquired that is shared by selective label images. Artery-selective imaging is possible by geometrically changing the position of the labeling focus to more than one artery of interest during measurement. The presented approach is compared to conventional super-selective imaging in terms of its labeling efficiency inside and outside the labeling focus using numerical simulations and in vivo measurements. Additionally, the signal-to-noise ratios of the images are compared to non-selective ASL angiography and analyzed using a two-way ANOVA test and calculating the Pearson's correlation coefficients.
Results The results indicate that the labeling efficiency is not reduced within the labeled artery, but can increase as a function of distance to the artery of interest when compared to conventional super-selective ASL. In the final images, no statistically significant difference of image quality can be observed while the acquisition duration could be reduced when the major brain feeding arteries are being tagged.
Conclusion Using super-selective arterial spin labeling, a single non-selective control acquisition suffices for reconstructing selective angiograms of the cerebral vasculature, thereby accelerating image acquisition of the major intracranial arteries without notable loss of information.

Keywords Selective · Angiography · Arterial spin labeling · Cycled

Introduction

Non-contrast enhanced magnetic resonance angiography (NCE-MRA) methods are commonly used for the detailed anatomical investigation of the intracranial arterial status and its function. Examples include time-of-flight (TOF) or phase-contrast angiography (PCA), but these are often limited, as only the whole cerebral vasculature can be depicted at once [1–3]. Therefore, drawing conclusions about single arteries can be impeded, but would be important for instance in the evaluation of individual feeding arteries of tumors or arterio-venous malformations (AVM). Using MRI, the application of specialized approaches, such as selective arterial spin labeling (ASL) methods, allow for the visualization of individual arteries, e.g., the major brain feeding vessels and even small intracranial branches [4–7].

Among different tagging approaches, pseudo-continuous ASL (pCASL) is often used for angiography [5, 8–10]. Furthermore, certain modifications of pCASL make it possible to create a labeling spot rather than a plane that allows for selectively labeling a single artery (super-selective ASL) [7]. This approach was already successfully applied for selective angiography measurements in volunteers and patients [8, 9]. Like most ASL techniques, pCASL relies on the acquisition of two images (label and control), which are subsequently subtracted so that only the difference signal of the arteries is visible in the final images. Investigations of the spin behavior in super-selective ASL revealed

✉ Thomas Lindner
Thomas.Lindner@uksh.de

[1] University Hospital Schleswig–Holstein, Campus Kiel, Clinic for Radiology and Neuroradiology, Arnold-Heller-Straße 3, 24105 Kiel, Germany

[2] Philips GmbH Innovative Technologies, Research Lab, Röntgenstraße 24-26, 22335 Hamburg, Germany

oscillations of the labeling efficiency outside the artery of interest [7]. Therefore, the label and control images should be acquired using the same geometrical position and identical sequence parameters to maximize labeling efficiency inside a selected vessel and minimize it outside the labeling focus. However, the acquisition of two corresponding label and control images for each selected artery can make the measurements in super-selective ASL time-consuming. Moreover, the measurements are performed separately for each artery of interest, increasing the risk for patient movement between the acquisitions. More time-efficient approaches were already proposed using pulsed ASL (PASL) or vessel-encoded pCASL (VEPCASL) to visualize individual perfusion territories or selected arteries. These are either based on dual-vessel labeling and subsequently combining the resulting images with a single control condition (PASL), or on calculating selective angiograms or flow territories by acquiring non-selective tag and control images alongside multi-vessel labeled images (VEPCASL) [4, 11, 12]. Other methods employ a rotating control condition or use an approach to tag the anterior and posterior circulation simultaneously using two labeling slabs [13, 14].

One advantage of super-selective pCASL compared to other approaches is the flexibility of positioning the labeling spot. For example, the arteries of interest do not need to have a sufficiently long straight segment in a single plane, but the labeling focus for each artery can be adapted to the different vessels individually, e.g., by tilting the labeling spot in arbitrary directions according to the course of the artery [4, 7]. Additionally, the size of the focus can be manually adjusted and thereby optimized with respect to individual vessel diameters [7]. Especially in patients with an altered vasculature, this can become an advantage compared to methods that apply large labeling slabs or require positioning a single labeling plane so that the blood in all arteries of interest will experience sufficient labeling. In some clinical applications, information about selected arteries only, rather than the whole vasculature, can be of interest. Furthermore, patients will have most likely already underwent non-selective angiography, e.g., time-of-flight (TOF) imaging. Usually, this makes it possible to gather a lot of information about a pathology. However, acquiring images of only the relevant arteries (e.g., just the left carotid and left vertebral artery) may be sufficient for a proper diagnosis. In multi-vessel tagging approaches, it is often required to perform many encoding cycles with respect to the number of supplying arteries in order to decode single arterial flow territories [4]. The aim of this work is to present a method of time-resolved artery-selective ASL angiography imaging that is based on super-selective pCASL, denoted as "cycled super-selective pCASL," as this approach allows for flexible positioning of the labeling spot on top of individual arteries, which has been demonstrated to be beneficial in patients with an altered vasculature [15]. To reduce scan time compared to the conventional super-selective approach, a single non-selective control condition is used [4, 11, 13]. However, compared to conventional super-selective ASL, using a non-matching control acquisition might increase the deviation between control and label image, leading to higher labeling efficiencies in non-selected vessels. To assess the feasibility of cycled super-selective ASL, numerical simulations of the labeling efficiency inside and outside a selected artery of interest are performed and validated in a volunteer study. Additionally, SNR measurements of the resulting angiograms are compared to conventional super-selective ASL and non-selective ASL, the latter being considered the gold-standard method of acquiring ASL angiograms in this study.

Methods

Numerical simulations and validation

To assess the feasibility of the proposed method, numerical simulations of the labeling efficiency were performed. These were conducted by numerically solving the Bloch equations over blood flow velocities of 1–60 cm/s, assuming laminar flow and a vessel diameter of 3.5 mm [7]. The simulation process assumed fully relaxed spins at the beginning of the experiment and took into account the inversion profile of the Hanning shaped RF pulses used during pCASL tagging. In-between two pulses, the phase change due to the perpendicular applied gradients was calculated. For each calculated velocity, this was repeated until the spins passed the simulated inversion slab. The pCASL parameters used were a flip angle of 18° with a pulse spacing of 1 ms. The mean tagging gradient was set to 0.6 mT/m and the maximum gradient amplitude to 6 mT/m. As relaxation parameter, T_1 and T_2 of blood were assumed to be 1650 and 100 ms, respectively.

For cycled super-selective ASL, super-selectivity was achieved using a gradient moment of 1.08 mT/m in anterior-posterior and right-left direction during the pCASL pulse train for the labeling condition, and with zero gradient moment in the control condition. For conventional super-selective ASL, the extra gradients were performed in both the label and control experiment [7]. To visualize the deviations in labeling efficiency over the distance to the tagged artery, the calculations were performed over a range of 0–60 mm. The simulations were then validated by acquiring images of five volunteers while shifting the labeling focus over the same distance in 5 mm increments away from the selected artery for both the super-selective and cycled super-selective approach using a labeling duration

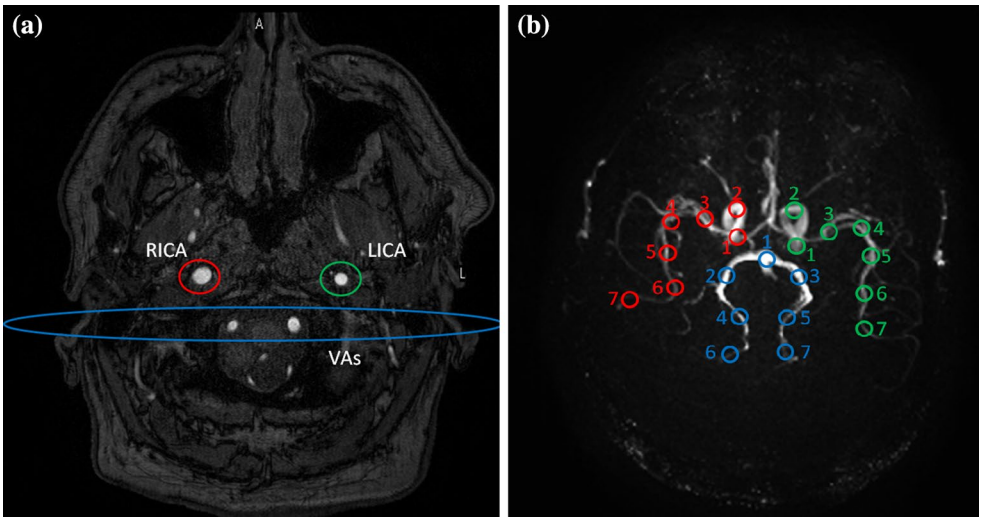

Fig. 1 **a** Planning of the individual acquisitions to obtain artery selective images. The right internal carotid artery (RICA) is tagged in acquisition 1 (*red*), the left internal carotid artery (LICA) in acquisition 2 (*green*) and both vertebral arteries (VAs) in acquisition 3 (*blue*). In the latter case, the gradient moments of the super-selective labeling gradients are adjusted to form an ellipsoid labeling focus [14]. Acquisition 4 (control condition) is performed without transversal gradients. **b** Representative locations for placing regions of interests (ROIs) for the SNR analysis

of 1000 ms without labeling delay. Image readout was performed using a 3D fast spoiled gradient echo sequence with a spatial resolution of 0.9×0.9 mm^2 and 20 slices with a thickness of 3 mm each. Additionally, a non-selective scan was performed using the same scan parameters.

The dependence of the labeling efficiency on the distance to the tagged artery was measured directly above the labeling plane using region of interest (ROI) analysis inside the arteries in the subtracted images of the cycled and the super-selective approach. The results were normalized with respect to the signal measured in the non-selective acquisition (Eq. 1). The labeling efficiency was thus calculated as

$$\text{Labeling efficiency} = \frac{(\text{SI}_{\text{control}} - \text{SI}_{\text{label}})_{\text{conventional/cycled}}}{(\text{SI}_{\text{control}} - \text{SI}_{\text{label}})_{\text{non-selective}}} \quad (1)$$

where SI denotes the signal intensity of the respective images [7].

Calculation of the subtraction angiograms

In non-selective and super-selective ASL, two images are acquired. The first (label) is subtracted from the second (control) to obtain the final artery-selective angiogram. The acquisitions of one pair of label and control images form one cycle. This has to be repeated for each artery in the case of conventional super-selective ASL.

In the presented approach of cycled super-selective ASL, one cycle is split into four individual acquisitions during the scan. One label acquisition is performed for each of the major arteries and a non-selective control condition is acquired for subsequent subtraction. In this method, the four acquisitions form one cycle. In this study, the left and right carotid arteries (LICA, RICA) and the vertebral arteries (VAs) were tagged selectively.

Subtraction of acquisition four (control) with each of the label acquisitions then results in the final angiographic images.

Magnetic resonance (MR) experiments

The data acquired for this study was part of a general protocol for MRI pulse-sequence development approved by the local ethical committee. All volunteers gave written informed consent before they underwent MR imaging. The study population included 13 healthy volunteers (eight women and five men, mean age 28.2 years) without any known history of vascular disease. All imaging experiments were performed on a Philips 3T Achieva MR scanner (Philips Healthcare, Best, The Netherlands) using a 32-channel receive head coil. To plan the selective ASL measurements, the information about the position of the arteries is obtained via a TOF angiography scan placed over the neck [9]. An example of the geometry used to tag the major arteries is given in Fig. 1a. A schematic overview of the pulse sequence is shown in Fig. 2.

In order to visualize the leading edge of the labeled blood bolus, the labeling duration was set to 400 ms and a 50 ms post labeling delay was used. WET presaturation pulses were applied prior to labeling to reduce static

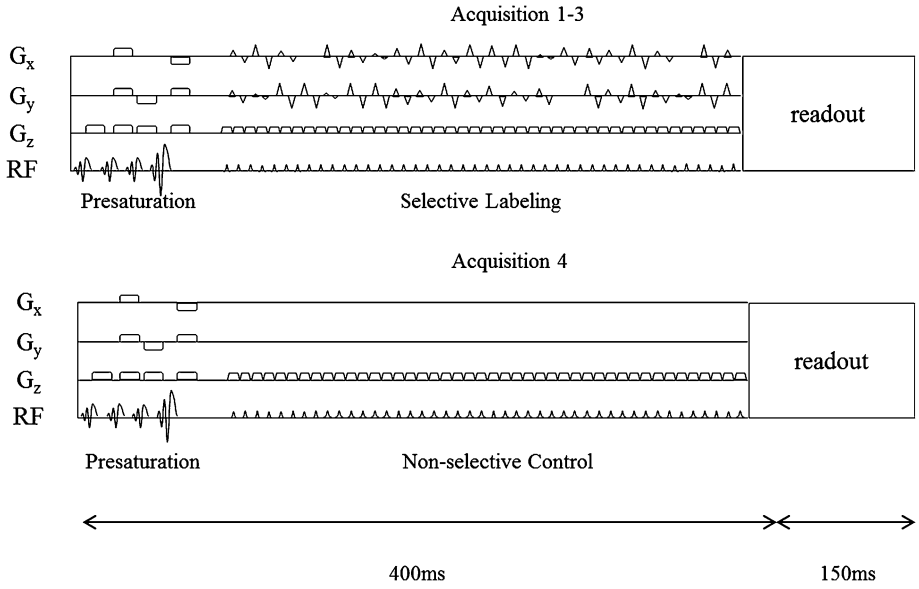

Fig. 2 Schematic sequence diagram for the acquisitions *1–3* and acquisition *4* in the presented method. The length of the labeling/control pulse train is displayed only partially. After presaturation of the static tissue, in acquisitions *1–3*, the extra gradients for the selective labeling method are applied, achieving tagging of a single artery. In acquisition *4* (control condition), no extra gradients are applied and the phase of every second RF pulse is shifted by 180° to achieve zero net inversion

Table 1 Total scan durations to acquire images of the three major arteries for the different tagging methods

Labeling type	Total duration (min)
non-selective ASL	05:08
super-selective ASL	15:24 (5:08 per artery)
Cycled super-selective ASL	10:17

tissue signal. For selective labeling of the ICAs, the additional gradient moments were adjusted to 1.08 mT/m in the anterior-posterior (Gx) and left–right (Gy) direction; for the VAs, the zeroth moment of the gradient in left–right direction was set to 0.1 mT/m to achieve an ellipsoid labeling focus, thus making it possible to label both VAs at the same time (Fig. 1a) [7, 15, 16]. Image acquisition was performed using a 3D fast spoiled gradient echo readout sequence and a flip angle of 10°. Each repetition of the label/control loop acquired 16 lines in k-space. Acquisition of the selective label images and the control image is performed in an interleaved way, meaning that after each partial k-space readout of one artery, a different labeled artery (or the control image) is acquired. This has the advantage of being more robust in terms of small continuous head movement of the patient's head, as the acquisitions are performed closer together in time [12]. The TR/TE was set to 7.9/3.7 ms and the acquisition matrix used was 240 × 240 with 0.9 mm^3 isotropic voxel size. 120 slices were acquired with a SENSE factor of three, covering a volume of 10.8 cm that displays the entire vasculature including and above the circle of Willis. Six consecutive time points after labeling were acquired with a temporal resolution of 150 ms in order to image the inflow of labeled blood. No cardiac triggering was performed. The total scan durations for the different approaches are summarized in Table 1. In one volunteer, the cycled super-selective approach was additionally performed above the CoW, namely in the anterior (ACA) and both middle cerebral arteries (MCAs) using the same ASL and readout parameter as described above, and compared to conventional super-selective ASL. The number of slices was halved to 60 and the stack placed directly above the super-selective tagging positions.

All images were exported and post-processed using Matlab R2013b (The Mathworks, Natick, MA). This included image subtraction and the generation of maximum intensity projections (MIPs). To obtain a holistic picture of the cerebral vasculature, the selective MIPs were also merged into a single color-encoded frame.

SNR measurements

To compare the SNR of the selective methods, the non-selective ASL angiography scan was considered the reference method, as the labeling efficiency can be expected to be more consistent across the volunteers [7]. To perform quantitative comparisons, the mean SNRs were calculated by performing ROI analysis using ImageJ (ImageJ, Bethesda, MD) and calculated using the formula:

$$\mathrm{SNR}_{\mathrm{mean}} = S_{\mathrm{mean}}/\sigma_{\mathrm{BG}} \quad (2)$$

where S_{mean} is the mean signal of the ROI covering the arteries and σ_{BG} is the standard deviation of the background signal [17].

The measurements were performed at seven defined locations in each of the major arteries for all acquired time points. These are presented schematically on a transversal MIP in Fig. 1b. The ROI was then copied to the other images of the same volunteer to avoid any misplacing or

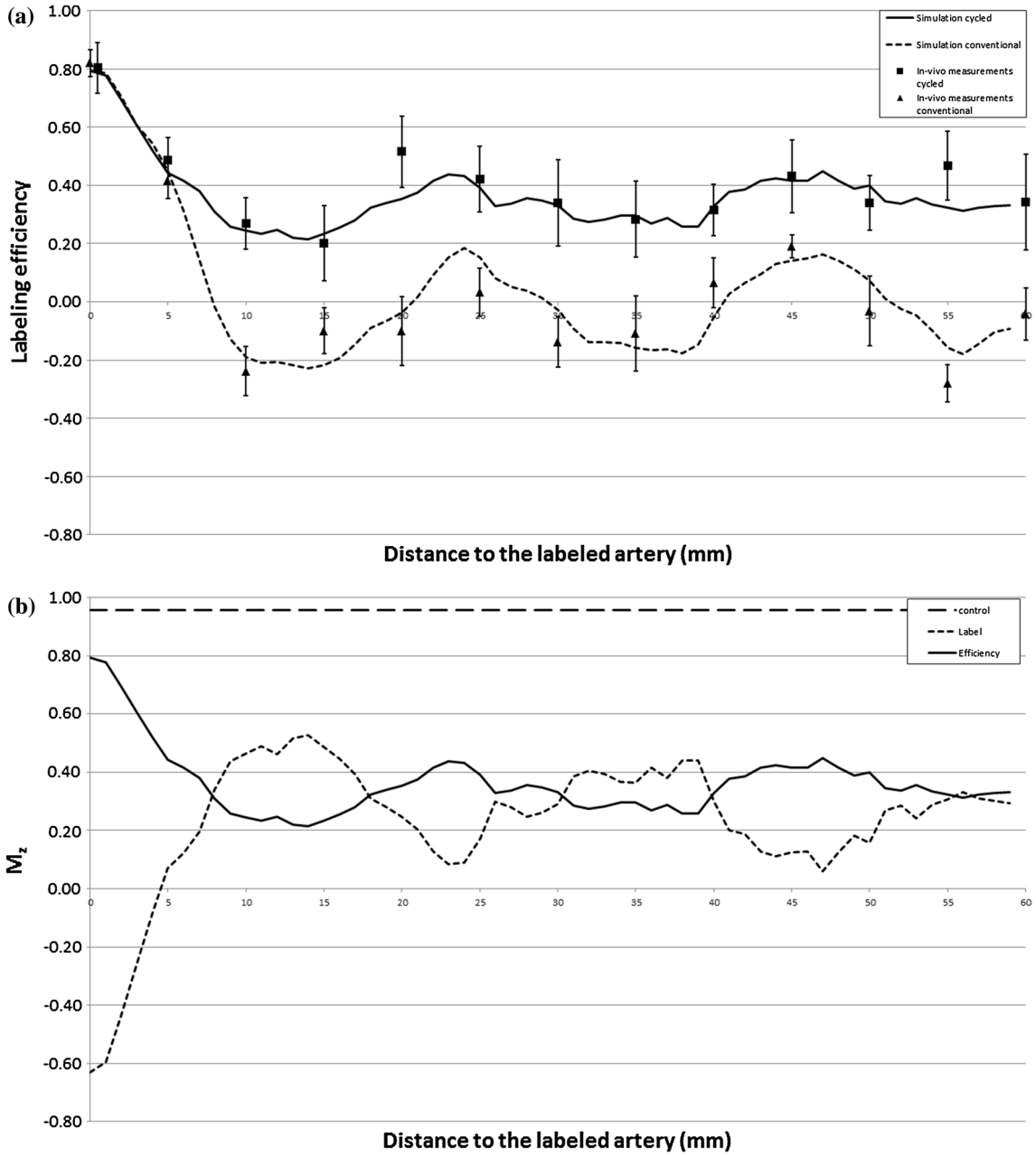

Fig. 3 **a** Simulated and measured labeling efficiencies as a function of distance to the selected artery for conventional and cycled super-selective ASL. *Error bars* of the measured data represent the standard deviation from acquisitions in five volunteers. Note that the result from the cycled method is shifted to the right at distance zero for better visualization. **b** Simulation of the labeling efficiency of cycled super-selective ASL in conjunction with the longitudinal magnetization values as a function of the distance to the labeled artery. Shown are the magnetic state of the control image (*dashed line*), of the label image (*dotted line*) and the resulting labeling efficiency as calculated in Eq. 1 (*solid line*)

contouring bias. Statistical analysis was performed using ANOVA testing to assess differences between the three methods [18]. A p value of 0.05 was considered as statistically significant. Additionally, the Pearson's correlation coefficient was calculated for all major arteries for the three methods. To assess similarity between the approaches, Bland–Altman plots were created considering non-selective ASL as the reference method [19].

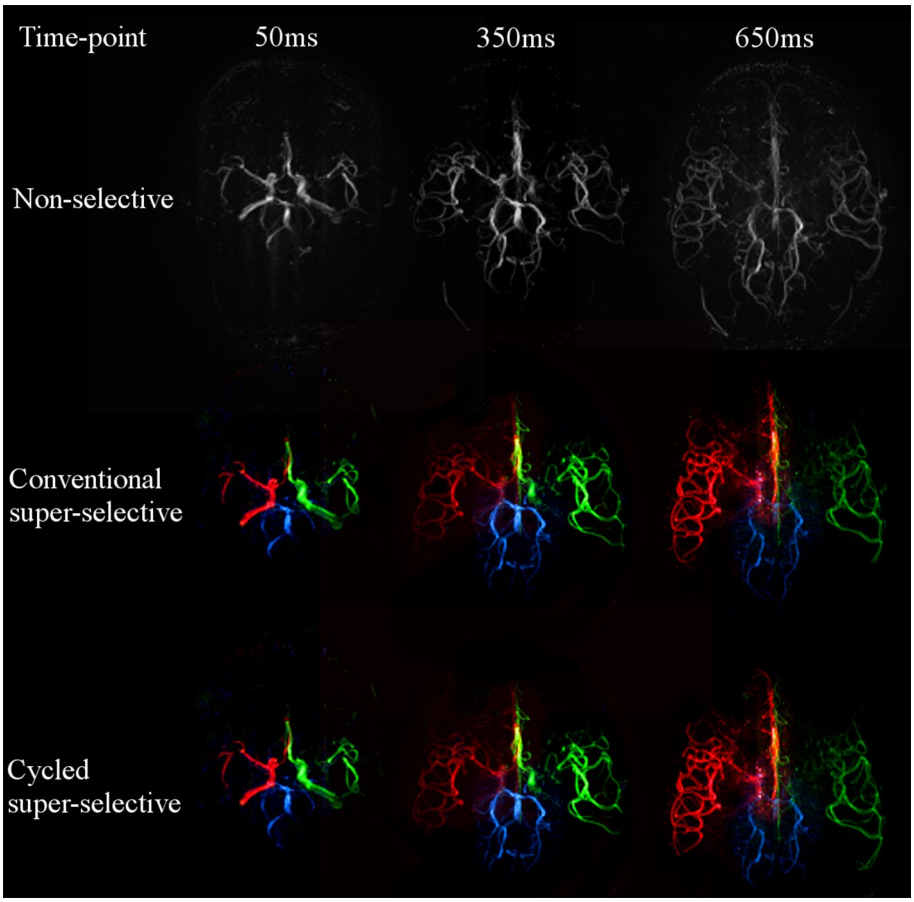

Fig. 4 Representative transversal maximum intensity projections of one volunteer for the three performed methods. Only the first, third and fifth time frame (50, 350 and 650 ms) are shown. The non-selective angiography presents all arteries during a single scan. The individually tagged major arteries in case of selective acquisitions are color-encoded, whereas the right ICA is displayed in *red*, the left ICA in *green* and the posterior circulation in *blue*

Results

Numerical simulations and validation

The results from the numerical simulations and the corresponding volunteer measurements are shown in Fig. 3. The simulated and measured labeling efficiencies for the super-selective approach are in concordance with the values presented in the original publication [7]. The results from the simulation of the cycled super-selective method indicate a higher labeling efficiency (oscillating between +20 and +40 %) as a function of the distance to the tagged artery, compared to conventional super-selective ASL having an oscillating efficiency between −20 and +20 %. The efficiency of both methods within approximately 3 mm from the labeling focus appears identical.

MR experiments

Image acquisition was performed successfully and all data sets could be used for the SNR measurements. Figure 4 shows representative MIPs of the final images of one volunteer after combining all vessels into a single color-encoded frame. An example of tagging smaller intracranial arteries above the circle of Willis is given in Fig. 5. Compared to conventional super-selective ASL (Fig. 5a), the cycled approach shows signal from the ACA when tagging the left MCA and vice versa (Fig. 5b). This was not observed on the right MCA.

SNR measurements

The SNR of non-selective, conventional super-selective and cycled super-selective ASL imaging compare similarly, which can be seen in the Bland–Altman plots (Fig. 6). Following statistical analysis, no trend between the tagged arteries could be observed. The ANOVA analysis yielded a p value of 0.51 for the RICA, 0.46 for the LICA and 0.55 for the posterior circulation indicating no statistically significant differences between the methods in terms of SNR. The calculated Pearson's correlation coefficients also show a high correlation ($\geq$0.78) between the methods and can be found in Table 2.

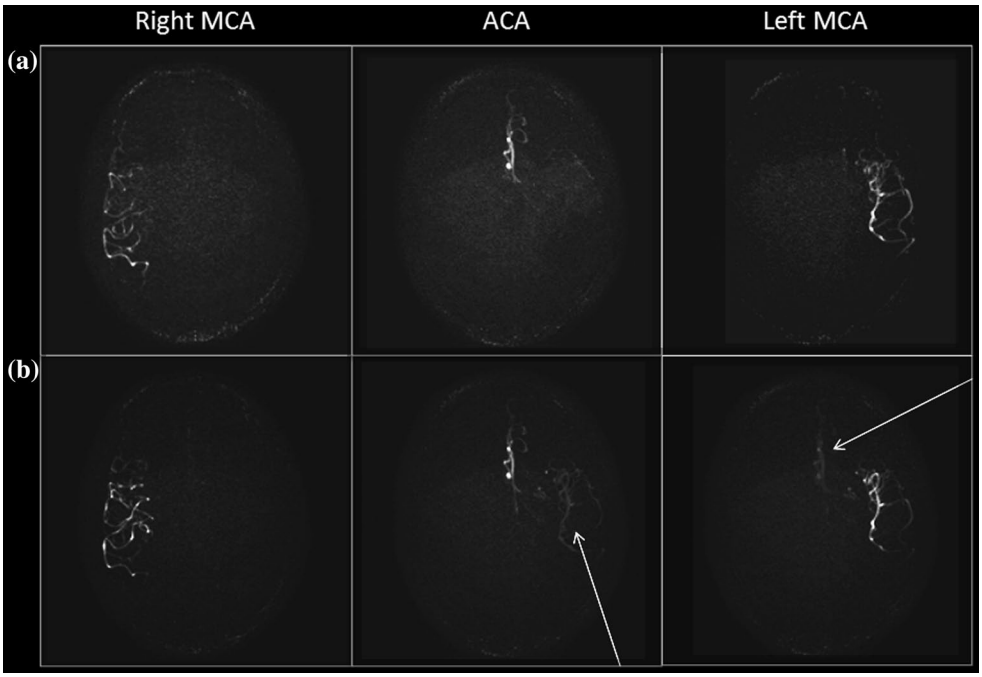

Fig. 5 Example of super-selective tagging above the circle of Willis using conventional super-selective (**a**) and cycled super-selective ASL (**b**). In **a**, no unwanted signal can be seen, while in **b** the left middle cerebral artery (MCA) is visible when the anterior cerebral artery (ACA) was tagged and vice versa. This could be explained using the simulations of the labeling efficiency presented in Fig. 3, as the right MCA had a distance of 16 mm (minimum) and the left of 21.4 mm (maximum) to the ACA

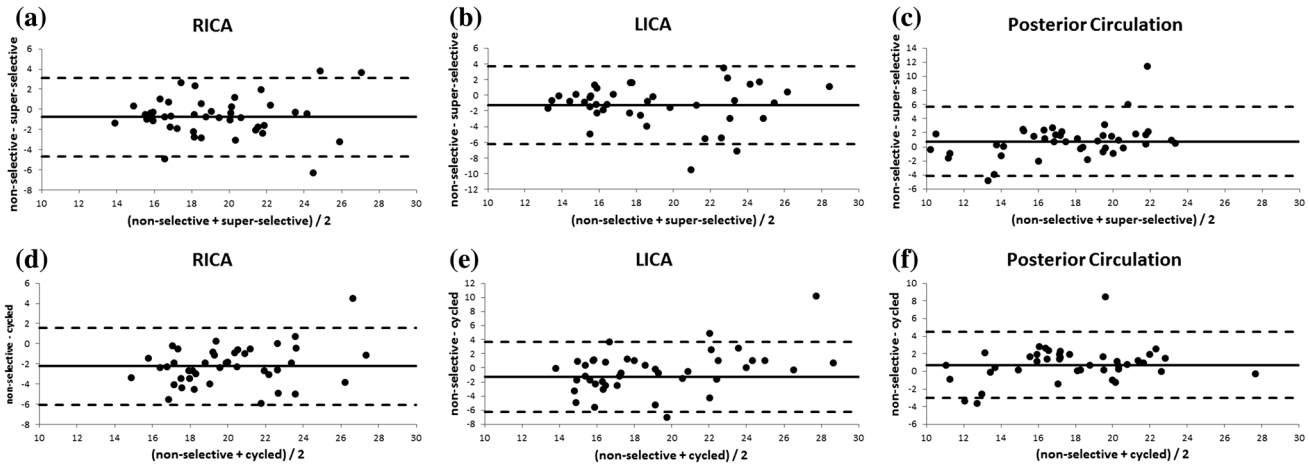

Fig. 6 Bland-Altman plots for the three evaluated methods with non-selective ASL being considered as the reference standard. Shown are the differences in SNR on the y-axis and the mean SNR on the x-axis. The upper and lower boundaries presented as dashed lines are the mean values ±2 times the standard deviation. The solid line is the mean difference of the methods. The results for the respective arteries for the conventional super-selective method are seen in plots **a**–**c**, and for the cycled super-selective method in **d**–**f**. The results indicate that the performance of both methods appears similar in terms of SNR as compared to non-selective pCASL

Table 2 Pearson's correlation coefficients of the SNR measurements visualized as correlation table for the three methods in the three major arteries that have been visualized

Visualized artery	Non-selective			Conventional			Cycled		
	RICA	LICA	VA	RICA	LICA	VA	RICA	LICA	VA
Non-selective	1	1	1						
Conventional	0.82	0.87	0.79	1	1	1			
Cycled	0.82	0.81	0.88	0.84	0.87	0.78	1	1	1

Discussion

In this study, an approach for the accelerated visualization of individual arteries in the cerebral vasculature, denoted as cycled super-selective pCASL, is proposed and evaluated in terms of SNR compared to the conventional super-selective and non-selective pCASL angiography approach. Generally, to obtain angiographic images using ASL, a label image has to be performed with a matching control image. These should have the same contrast properties, except for the magnetic state of the inflowing labeled blood in order to subtract the static background tissue as accurately as possible. In super-selective ASL, the additionally performed gradients perpendicular to the labeling plane could cause adverse effects, so that it is important to acquire a corresponding control condition, in which the same gradient pattern is used [7]. Influencing factors of the labeling efficiency are the gradient scheme, the geometrical position, as well as the strength of the additional gradients defining the size and shape of the labeling focus [7, 16].

The control condition in cycled super-selective ASL is obtained using a standard non-selective ASL control image, i.e., without the perpendicular gradients from the super-selective approach [7]. The effect of its use was evaluated in numerical simulations and in volunteer scans. The results from the volunteer study indicate no qualitative degradation of the images. In offsets below 3 mm, no deviations of the labeling efficiency within the artery of interest can be expected compared to conventional super-selective ASL (Fig. 3a). One limitation of the presented approach could be the increased labeling efficiency in the contralateral arteries. As the labeling efficiency decreases with increasing offset (from the tagged artery), in cases of a misplaced focus or patient movement, the efficiency can become the same as in one of the contralateral arteries, e.g., misplacement of 5 mm would yield the same efficiency as an artery with a distance of 23 mm (Fig. 3a). This could lead to unwanted signal in one or more of the non-tagged vessels, as no major deviations in the static tissue component can be expected. In the worst case (23 mm and 47 mm offset from the tagged artery), the unwanted signal component inside the contralateral artery can be approximately two-thirds of the tagged artery (Fig. 3b). In the situation of tagging the major arteries, maximum signal can arise in the contralateral carotid artery, resulting in approximately half the signal compared to the tagged artery. By selectively labeling intracranial arteries, this problem is more likely to appear as presented in Fig. 5. In this particular volunteer, a distance of 16 mm was measured between the labeling spot on top of the right MCA and the right ACA. Comparing these results with the performed simulations, a minimum of labeling efficiency remains in the right ACA when the labeling spot is positioned over the right MCA. On the left side of the brain, MCA and ACA vessels were separated by 21.4 mm. This distance results in a maximum of the labeling efficiency outside of the labeling spot and explains the increased signal in the left MCA when the left ACA is selectively labeled and vice versa. The distance to the right MCA appears more favorable regarding the residual labeling efficiency and presents similar images when compared to conventional super-selective ASL. A potential remedy would be changing the position of the tagging plane so that the labeling efficiency is minimal according to the simulation results. This is possible using super-selective ASL, as the position and angulation can be adjusted individually. Another possibility would be an advanced technique of super-selective ASL that does not result in an oscillating labeling efficiency outside the labeling spot, thereby reducing unwanted signal contributions, e.g., by using a fully randomized instead of a pseudo-randomized pattern. Theoretically, the presented approach is not limited in the number of arteries to be imaged during one measurement. As super-selective tagging already showed its potential to visualize individual branches of the intracranial arteries separated less than 7 mm, cycled super-selective ASL can most likely also be adapted to image these arteries while the presented calculation scheme can be applied accordingly [7, 20].

Another approach to evaluate image quality could be ratings with respect to visualization and assessment of individual arterial segments. This can be considered for a more detailed analysis of image quality, in order to compare the potential of the proposed approaches with established imaging methods [8, 21, 22].

Compared to non-selective acquisitions, vessel-selective tagging approaches generally increase the total imaging time linear to the number of tagged arteries. On the other hand, these techniques offer information about individually selected arteries. When the aim is to selectively visualize a larger number of arteries, this might lead to prolonged overall scan durations and increase the possibility of patient movement in-between two consecutive scans, thus degrading the quality of the final images. In recent years, several strategies to efficiently acquire images of multiple labeled arteries have been presented [4, 11, 23]. One study using VEPCASL for angiographic imaging is based on six individual acquisitions forming one cycle [12]. For acquiring images of the internal carotids as well as the individual vertebral arteries, this strategy is SNR optimal as all vessels are in the tag and control condition equally often [12]. To acquire a single image from the posterior circulation (as also used in this study), the same strategy can be performed to tag the basilar rather than the vertebral artery, which would decrease imaging time, but encoding those three vessels would still need five acquisitions including the “tag all” and “control all” images. Compared to other

approaches, e.g., VEPCASL, in the presented approach, no "tag all vessels" acquisition is performed and the calculations are not based on a probabilistic model [12]. Therefore, considering total image acquisition time, with comparable sequence parameters, the cycled super-selective approach would then result in shorter scan times. Despite the lower expected SNR, the results from this study indicate that images of sufficiently high SNR can be obtained. A different approach, also based on four acquisitions, was presented for regional perfusion imaging using pulsed ASL. In this, two post-processing steps are necessary for the reconstruction of artery-selective images that might be impeded in patient cases with altered vasculature or mixed territories.

Another advantage of using single-artery labeling is that labeling spot can be adapted in size and position to each of the arteries of interest individually and the foci do not have to lie within a single plane, but can be distributed over the whole volume within a single scan [4, 7, 20]. This becomes especially advantageous in tagging smaller intracranial arteries, as it is unlikely to have a sufficiently straight segment with the same orientation of each artery within the same plane, that is necessary in other approaches [12, 20]. The only restriction of the presented method is that none of the labeling foci should be inside the imaging volume to avoid artifacts due to the super-selective tagging gradients. The labeling duration, delay and acquisition durations have to be adapted accordingly.

Compared to conventional super-selective pCASL, the acquisition time for the presented method is decreased by one-third (Table 1), while still obtaining information about single arteries is possible. Therefore, the presented approach may also represent an alternative to be used for clinical imaging procedures as compared to other selective ASL NCE-MRA acquisitions, which are limited by either long acquisition times or limited spatial coverage [21–25]. Another important parameter regarding image acquisition time is the number of k-space lines that are read out in each label/control loop. This parameter was chosen based on previous knowledge finding a compromise between acquisitions duration and loss of signal due to spoiled readout, as acquiring more lines would lead to shorter scan times, but at the expense of image quality [9]. To acquire one image, 135 repetitions of each the label and the control condition were performed in non-selective and conventional super-selective ASL. Conventional super-selective thereby needs to acquire a total of 810 loops, while the cycled approach needs 540.

As in cycled super-selective ASL, image post-processing is performed using standard image subtraction as for conventional non-selective or super-selective ASL, in cases of a single corrupted acquisition, this might still allow to reconstruct images of the remaining arteries. This is contrary to other encoding approaches, having two of three vessels simultaneously in the label state in each acquisition [4, 11]. Using the super-selective tagging approach, also multi-vessel labeling is possible and could be used accordingly to perform Hadamard type decoding [4, 11, 12, 16]. This might pose an alternative to be used for labeling three or more vessels in healthy volunteers, especially when all arteries are of interest, but this might be impeded in pathologic cases with tortuous vasculatures or in tagging smaller arteries above the Circle of Willis due to their closer spacing and the higher number of individual arteries to be tagged.

In conventional super-selective ASL, using one angiography scan for planning could lead to inter-scan movement, potentially misplacing the focus with respect to the artery of interest. This can only be circumvented by acquiring an angiography scan for each artery of interest separately before starting the measurement, which further increases overall scan time [20]. In the presented approach, only one scan for planning needs to be performed for all arteries to be acquired. Acquiring the images in an interleaved fashion, rather than successively, reduces the possibility of a systematic shift of the patient's head position and allows for more accurate subtraction than acquiring the selective images (and the control image) one by one [12]. Movement during the scan, as the cycled approach takes in total approximately 10 min, or motion between planning and acquisition, however, are still persisting limitations. To counteract possibly occurring intra-scan movement of the patients, real time motion trackers can be performed [26]. These can be implemented using recently developed strategies, e.g., within the short post-labeling delay after labeling, so that the initial scan time will not be prolonged [27].

The presented method should be further evaluated in cerebrovascular diseases, in order to prove its applicability and reproducibility in the clinical setting.

Conclusion

The presented method of cycled super-selective ASL allows for the NCE-MRA acquisition of individually selected intracranial arteries within a single scan and without notable loss of SNR when the major brain feeding arteries are being tagged. It could be proven that the acquisition of a single non-selective control image leads to shorter scan times compared to the conventional label-control acquisition in super-selective ASL.

Acknowledgments This work was supported by funding of the German Research Foundation (DFG), Grant Number: JA 875/4-1.

Compliance with ethical standards

Funding The study was as part of the project funded by the German Research Foundation (DFG) with the grant number JA 875/4-1. The content of the article was not influenced by the funding source. No other external funding was involved in the study.

Conflict of interest Michael Helle is an employee at Philips GmbH Innovative Technologies, Research Laboratories in Hamburg, Germany.

Ethical standards The study was conducted in accordance to the ethical standards of the local ethical committee (Medical University of Kiel) and with the Helsinki Declaration of 1975, as revised in 2000.

Informed consent All volunteers gave written informed consent prior to be included in the study.

References

1. MacDonald ME, Frayne R (2015) Cerebrovascular MRI: a review of state-of-the-art approaches, methods and techniques. NMR Biomed 28:767–791
2. Nishimura DG (1990) Time-of-flight MR angiography. Magn Reson Med 14:194–201
3. Dumoulin CL, Souza SP, Walker MF, Wagle W (1989) Three-dimensional phase contrast angiography. Magn Reson Med 9:139–149
4. Wong EC (2007) Vessel-encoded arterial spin-labeling using pseudocontinuous tagging. Magn Reson Med 58:1086–1091
5. Nakamura M, Yoneyama M, Tabuchi T, Takemura A, Obara M, Tatsuno S, Sawano S (2013) Vessel-selective, non-contrast enhanced, time-resolved MR angiography with vessel-selective arterial spin labeling technique (CINEMA-SELECT) in intracranial arteries. Radiol Phys Technol 6:327–334
6. Robson PM, Dai W, Shankaranarayanan A, Rofsky NM, Alsop DC (2010) Time-resolved vessel-selective digital subtraction MR angiography of the cerebral vasculature with arterial spin labeling. Radiology 257:507–515
7. Helle M, Norris DG, Rüfer S, Alfke K, Jansen O, van Osch MJ (2010) Superselective pseudocontinuous arterial spin labeling. Magn Reson Med 64:777–786
8. Jensen-Kondering U, Lindner T, van Osch MJ, Rohr A, Jansen O, Helle M. Superselective pseudo-continuous arterial spin labeling angiography. doi:10.1016/j.ejrad.2015.05.034
9. Lindner T, Jensen-Kondering U, van Osch MJ, Jansen O, Helle M (2015) 3D time-resolved vessel-selective angiography based on pseudo-continuous arterial spin labeling. Magn Reson Imaging 33:840–846
10. Dai W, Garcia D, de Bazelaire C, Alsop DC (2008) Continuous flow-driven inversion for arterial spin labeling using pulsed radio frequency and gradient fields. Magn Reson Med 60(6):1488–1497. doi:10.1002/mrm.21790
11. Günther M (2006) Efficient visualization of vascular territories in the human brain by cycled arterial spin labeling MRI. Magn Reson Med 56:671–675
12. Okell TW, Chappell MA, Woolrich MW, Günther M, Feinberg DA, Jezzard P (2010) Vessel-encoded dynamic magnetic resonance angiography using arterial spin labeling. Magn Reson Med 64:430–438
13. Kamano H, Yoshiura T, Hiwatashi A, Yamashita K, Takayama Y, Nagao E, Sagiyama K, Zimine I, Honda H (2012) Accelerated territorial arterial spin labeling based on shared rotating control acquisition: an observer study for validation. Neuroradiology 54:65–71
14. Zimine I, Petersen ET, Golay X (2006) Dual vessel arterial spin labeling scheme for regional perfusion imaging. Magn Reson Med 56:1140–1144
15. Helle M, Rüfer S, van Osch MJ, Nabavi A, Alfke K, Norris DG, Jansen O (2013) Superselective arterial spin labeling applied for flow territory mapping in various cerebrovascular diseases. J Magn Reson Imaging 38:496–503
16. Helle M, Rüfer S, van Osch MJ, Jansen O, Norris DG (2012) Selective multivessel labeling approach for perfusion territory imaging in pseudo-continuous arterial spin labeling. Magn Reson Med 68:214–219
17. Firbank MJ, Coulthard A, Harrison RM, Williams ED (1999) A comparison of two methods for measuring the signal to noise ratio on MR images. Phys Med Biol 44(12):N261–N264
18. Fujikoshi Y (1993) Two-way ANOVA models with unbalanced data. Discr Math 116:315–334
19. Bland JM (1986) Altman DG Statistical methods for assessing agreement between two methods of clinical measurement. Lancet 8:307–310
20. Wong EC, Guo J (2012) Blind detection of vascular sources and territories using random vessel encoded arterial spin labeling. Magn Reson Matter Phy 25:95–101
21. Yan L, Wang S, Zhuo Y, Wolf RL, Stiefel MF, An J, Ye Y, Zhang Q, Melhem ER, Wang DJ (2010) Unenhanced dynamic MR angiography: high spatial and temporal resolution by using true FISP-based spin tagging with alternating radiofrequency. Radiology 256(1):270–279
22. Robson PM, Dai W, Shankaranarayanan A, Rofsky NM, Alsop DC (2010) Time-resolved vessel-selective digital subtraction MR angiography of the cerebral vasculature with arterial spin labeling. Radiology 257(2):507–515
23. Hartkamp NS, Petersen ET, De Vis JB, Bokkers RP, Hendrikse J (2013) Mapping of cerebral perfusion territories using territorial arterial spin labeling: techniques and clinical application. NMR Biomed 26(8):901–912
24. Hori M, Aoki S, Oishi H, Nakanishi A, Shimoji K, Kamagata K, Houshito H, Kuwatsuru R, Arai H (2011) Utility of time-resolved three-dimensional magnetic resonance digital subtraction angiography without contrast material for assessment of intracranial dural arterio-venous fistula. Acta Radiol 52(7):808–812
25. Iryo Y, Hirai T, Kai Y, Nakamura M, Shigematsu Y, Kitajima M, Azuma M, Komi M, Morita K, Yamashita Y (2014) Intracranial dural arteriovenous fistulas: evaluation with 3-T four-dimensional MR angiography using arterial spin labeling. Radiology 271(1):193–199
26. Zun Z, Shankaranarayanan A, Zaharchuk G (2014) Pseudocontinuous arterial spin labeling with prospective motion correction (PCASL-PROMO). Magn Reson Med 72:1049–1056
27. Helle M, Koken P, Sénégas J (2015) Improving motion robustness of pseudo-continuous arterial spin labeling by using real-time motion correction. Proc Intl Soc Magn Reson Med Toronto, ON, Canada. Abstract 0270